SPECIAL ISSUE ARTICLE



Development of a highly mobile and versatile large MA-XRF scanner for in situ analyses of painted work of arts

Emeline Pouyet¹ | Nicholas Barbi² | Henry Chopp³ | Owen Healy² |
Aggelos Katsaggelos³ | Sophia Moak¹ | Rick Mott⁴ | Marc Vermeulen¹ |
Marc Walton¹

Correspondence

Marc Walton, Center for Scientific Studies in the Arts Northwestern University, Evanston, IL.

Email: marc.walton@northwestern.edu

Funding information

Andrew W. Mellon Foundation; Northwestern University A new portable macro X-ray fluorescence scanner has been specifically designed for in situ, real-time elemental mapping of large painted surfaces. This system allows scanning $80 \times 80 \times 20 \text{ cm}^3$ along the X, Z, and Y directions, respectively, with adaptive beam size at the energy of the Rh Ka-line. The detection system consists of a 50 mm^2 active area detector coupled to a CUBE pre-amplifier and to the DANTE digital pulse processor (DPP) with adaptive shaping time. The system is controlled with a custom software including a graphical user interface (GUI) programmed in Python for real-time control of the stage, DPP, and camera of the scanner. This system allows considering new ways of sampling the object surface than the usual raster scanning in serpentine as well as a live elaboration of X-ray data; technical details and performances of the scanner are presented in this paper together with an example of its application to investigate painted surface, illustrating the value of the developed instrument.

1 | INTRODUCTION

Pigment identification is used by conservation scientists to elucidate artist/workshop use of materials, to understand how a painted surface has altered over time informing how an artwork is to be conserved, and, lastly, to identify anachronistic uses of materials that could be associated with either fakes and forgeries or associated with past restoration. A primary tool for these tasks is macro X-ray fluorescence (MA-XRF), a non-invasive method that has become common place in cultural heritage to examine how elements related to various pigments are distributed across a painted surface. [1,2] Recently, numerous instrument designs have been developed in an effort to cope with challenges associated with analyzing painted supports, for example, limited access to the object, and the high complexity and heterogeneity of the artifact at multiple scales.[3-11]

At the Northwestern University/Art Institute of Chicago Center for Scientific Studies in the Arts, object-based and object-inspired scientific research is performed on collections to advance the role of science within art history, curatorial scholarship, archaeology, and conservation. The Center utilizes a variety of transportable and non-invasive instruments, such as MA-XRF, reflectance imaging spectroscopy (RIS), optical coherent tomography, and Fourier transform infrared spectroscopy in reflectance mode. Among these methods, MA-XRF has become a key technique applied in most of the research projects undertaken by the Center. Originally, MA-XRF measurements were performed using a commercially available instrument, XGLab's ELIO (Milan, Italy), which has a nominal 1-mm spot size capable of on-tripod smallarea scanning $(10 \times 10 \text{ cm}^2)$. In addition, to map larger area objects, the ELIO analysis head was connected to an inexpensive scanning gantry, built in-house, controlled

¹Center for Scientific Studies in the Arts Northwestern University, Evanston, Illinois

²ON Science LLC, Sarasota, Florida

³Department of Electrical Engineering, Northwestern University, Evanston, Illinois

⁴PulseTor LLC, Pennington, New Jersey

by a microprocessor board to provide high precision positioning. Unlike commercial XRF scanning instruments, this system was portable and allowed for data to be collected from painted 2D objects in several cultural institutions across North America, including La Miséreuse accroupie (1902) and La Soupe (1903), both blue period paintings by Pablo Picasso housed at the Art Gallery of Ontario (AGO).^[12]

Despite being highly portable, the ELIO gantry system presents an inherent limitation in spatial resolution due to its 1-mm spot size. To overcome this limitation, we developed novel approaches to fuse data collected from the ELIO gantry with higher resolution imaging techniques such as RIS. This strategy has proven successful for imaging writing in historical manuscripts, ^[13] for instance, and can be applied to similar materials and techniques. However, fusion methods may not be universally successful for the analysis of more complex paintings with mixtures of pigments. Therefore, to improve spatial resolution, speed of acquisition, and portability, a new MA-XRF system has been designed and built.

The main requirements of our system were the following: (a) a large scanning area that can accommodate medium-sized paintings with micrometer resolution and repeatability; (b) high portability to accommodate transportation worldwide within a short period of time; (c) straightforward mounting and dismounting of the equipment; and (d) versatility, in particular with respect to the focusing optics and acquisition mode. The described system meets these requirements with scanning dimensions of $80 \times 80 \times 20$ cm³ along the X, Z, and Y directions, respectively. The detection system consists of a 50 mm² active area detector coupled to a CUBE pre-amplifier and a DANTE digital pulse processor with adaptive pulse shaping. Recent results obtained on reference material and a historical illuminated manuscript are described to present the potential of the equipment.

2 | TECHNICAL CHARACTERISTICS OF THE SCANNER

The MA-XRF system is presented in Figure 1. The X-ray source, XRF detection system, and visible camera are incorporated into a unit termed the 'XRF head' (Figure 1a, c). The XRF head is composed of a 12 W Rh-target X-ray tube (MOXTEK Inc., Orem, UT) coupled to a removable polycapillary optic (XOS Inc, East Greenbush, NY). As shown in Figure 2a, a beam diameter of 99.5 µm was measured at theoretical focal point (f = 4.8 cm) by a knife-edge scan across the direct incident beam while monitoring the Rh Kα-line. While the geometric divergence of 0.5° was determined for this optic from its output size, beam diameters were also experimentally recorded at a variety of focal distances using knife-edge scans as presented in Figure 2b. Since it is well known that polycapillary optics are achromatic, these figures of merits for the beam are expected to change dependent on the energy range being monitored.

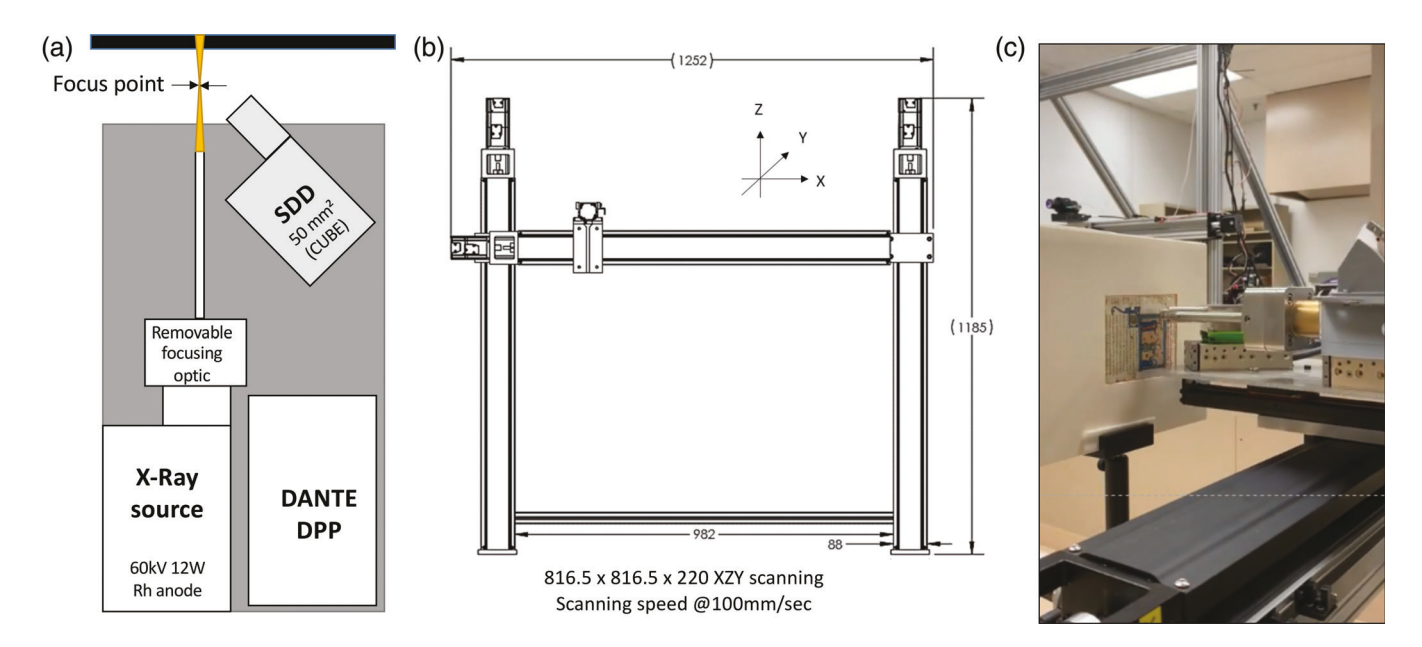


FIGURE 1 (a) Schematic view of the MA-XRF head assembly and geometry; (b) Mechanical drawing of the scanning stage allowing motion of $816.5 \times 816.5 \times 220$ mm in X, Z, and Y direction, respectively; (c) Visible picture of the system in use during the scan of the historical example presented hereby

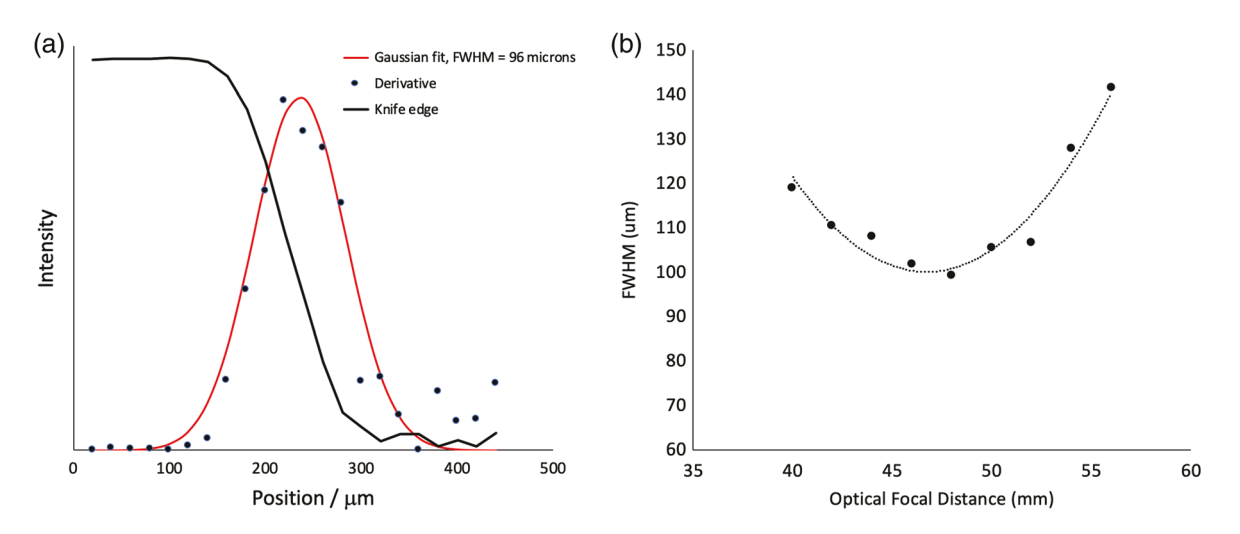


FIGURE 2 (a) Knife-edge scan at Rh K α -line demonstrating a beam diameter of 96 μ m at the theoretical focal distance of 4.8 cm. (b) Divergence of beam diameter measured at multiple distances

The polycapillary focusing optic was designed to be dismountable from the source to accommodate a larger pinhole or collimating system when larger spot sizes, higher count rates, or high Z elements are desired. X-rays are detected by means of a 50 mm² active collimated area Silicon Drift Detector (SDD, Bruker Nano Analytics), equipped with a CUBE preamplifier. [14] The detection module is read out by a newly designed digital pulse processor (DANTE DPP, Bruker Nano Analytics) characterized by excellent noise and high count-rate performance, and real-time data transmission capability for on-the-fly data collection. [15] The energy resolution at the Mn-Kα line is 132 eV for 100 kcps output count rate (OCR). The system can process an input count rate (ICR) of up to 1.5 million counts/sec yielding an OCR of 700 kcps, using adaptive pulse shaping time and yielding an energy resolution of <140 eV at Mn-Kα. The adaptive shaping permits operation at low dead times with minimal loss of resolution (411 kcps ICR, 328 kcps OCR, 134 eV) providing almost half the maximum throughput with 75% lower tube current. The X-ray source and detector operate in a 90-45 geometry, and are each mounted translation stages using 3D printed parts to optimize the detector and source alignment. Additionally, a FLIR camera (Blackfly S 20 MegaPixel) is used to position the sample at the polycapillary focus.

The XRF head is moved during the scanning by means of a custom commercial three-axis system mounted on a lightweight wheeled trolley (HIWIN, Huntley, IL), illustrated in Figure 1b. The scanning system consists of three linear stages allowing a travel range of 84 cm, 84 cm, and 20 cm along the X, Z, and Y directions, respectively. A laser interferometer was used to test the lead accuracy of the individual axes, resulting

into a 10 ± 1 µm accuracy over the whole travel range available in X and Z. This accuracy was maintained while scanning continuously at a speed and acceleration of up to 600 mm/sec and 300 mm/sec², respectively. The system operates in non-contact mode with about 10 mm of distance from the analyzed object (effective distance between the instrument head mechanics and the sample in optimal focusing position). With a total weight of 60 kg, stages, trolley, and XRF head can be easily transported and assembled for in situ experiments.

The software consists of a custom Python-based graphical user interface that controls the HIWIN stage and the Dante pulse processor. The software performs a raster scan parameterized by a step size, start/stop position, and per point dwell time inputs. A hardware trigger from the motor system to the DPP allows the DPP to produce a new spectrum at each trigger. For serpentine raster scanning, it triggers at the edge (start and end) of each pixel. The spectrum between triggers is the spectrum for that pixel. This approach allows non-raster segment scanning as well, for which a trigger is sent every 25 ms, yielding a motor position at each trigger and thus the position of each spectrum. The continuous stream of X-ray events from the DPP is processed in real time, which allows a live display of the elemental maps and spectra of interest defined by the users through the GUI during the scan.

3 | EXPERIMENTAL

The sensitivity and limit of detection of the system were determined from the spectrum acquired on the Standard Reference Material (SRM) 610 Trace elements,

manufactured by the National Institute of Standards and Technology (NIST). The spectrum was acquired for 500 ms real time at tube settings of 50 kV and 0.24 mA, without a filter, in air, and at the focal distance of 4.8 mm. The reference material is a 1-mm-thick glass disc containing a broad range of elements at a nominal concentration of 500 ppm.

The sensitivity (S) and limits of detection (LOD) of the system normalized for 1 s were calculated by means of Equations (1) and (2):

$$S_i = \frac{N_i}{C_i \times t} \tag{1}$$

$$LOD = 3 \times \frac{\sqrt{N_{\text{back}}}}{\sqrt{N_i}} \times C_i \times \sqrt{t}$$
 (2)

where N_i is the net count of the fluorescence peak of element i, C_i is the concentration of this element in the standard, t is the measurement time, and N_{back} is the

intensity of the background below the peak of the element (four sigma of the Gaussian function fitted to the peak were taken as the background width).

Similar to other commercial and in-house systems, the MA-XRF system aims at acquiring elemental distributions representative of concentrations of several mass percent with dwell times below 1 s. [3,7]. Figure 3a,b summarizes the chemical sensitivity and detection limits for the K-lines of elements detected in the corresponding standard. For the energy region around 3 keV, the sensitivity is above 100 cps/mg/g with a corresponding detection limit of about 70 ppm. A value of about 800–1,600 cps/mg/g was obtained for chemical elements with atomic numbers in the interval between 25 and 40. This allows for a limit of detection of about 30 ppm for elements with atomic numbers in this range. Chemical elements from Sb (Z 51) to Ba (Z 56) present a chemical sensitivity of some tens of counts per second due to the low transmission of the focusing optic at high energies. This inherent limitation of polycapillary optic therefore

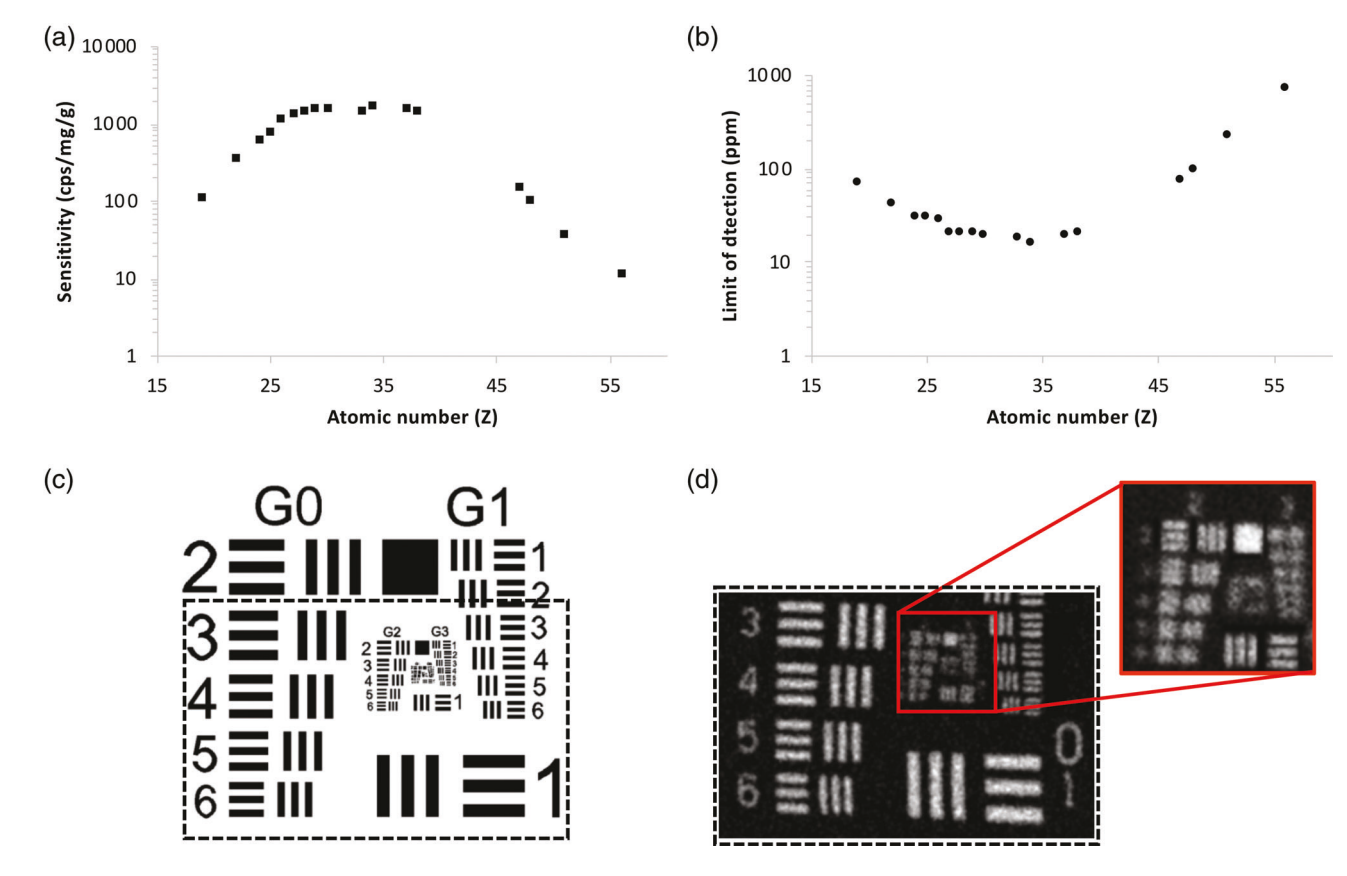


FIGURE 3 (a) K-line sensitivity for the elements K (Z = 19) to Ba (Z = 56) of the system at 50 kV and 0.24 mA; (b) K-line limit of detection for the elements K (Z = 19) to Ba (Z = 56) of the system at 50 kV and 0.24 mA; (c) Groundtruth Airforce USAF 1951 pattern, the slotted line square represents the area scanned by the MA-XRF instrument using a 70 μ m step size and 0.3 s dwell time and presented in (d) the Cr map of the USAF1951 resolution test target; the area highlighted in red corresponds to the central area of the target with higher spatial resolution, highlighting that the last resolved line pairs of the pattern are the one of group 2 element 3 (corresponding to a spatial resolution of 99 μ m)

means that high Z elements can only be investigated by using their L-lines.

The USAF1951 (chromium positive) resolution test target was used to determine the lateral resolution of the device as shown in Figure 3c,d. This target is designed to monitor lateral and horizontal resolutions resolvable by

microscopic systems with reference patterns spaced at known distances. The USAF-1951 test target presents a pattern composed by reference lines with defined spacing. The lines groups are repeated with dimensions ranging from 1 mm to 4 μ m (Figure 3c). The lateral resolution has been calculated by a step-by-step mapping of the

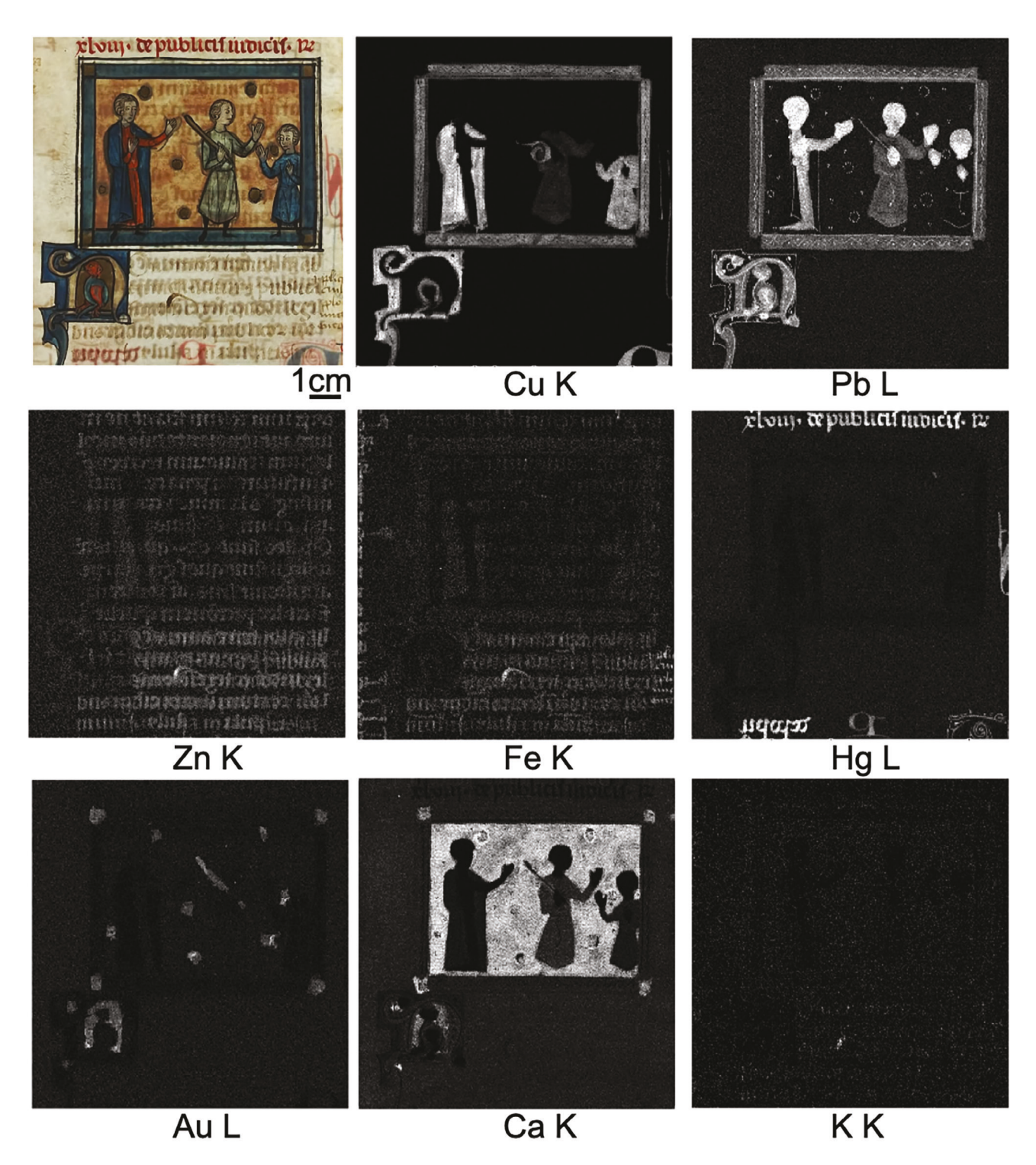


FIGURE 4 Elemental images of the illumination of a juridical manuscript fragment. MA-XRF acquisition was performed with a 300 µm pixel size, 100 ms dwell time for a total scan time of 110 min [Correction added on 12 August 2020, after first online publication: The part labels of the bottom row of Figure 4 had been omitted and were restored.]

central area of the target where higher resolution power is needed for resolving the pattern. Here, the USAF1951 sample was scanned with a 70 μ m step size and 0.3 s dwell-time while monitoring the chromium K α -line (Figure 3d). The system is able to resolve the bars in group 2, element 3 which corresponds to a lateral resolution of about 99 μ m which is near the beam size minimum determined by the knife-edge scan. With a Line Pairs (LP) per millimeter of 5.04 for the group 2 and element 3, the resolution was obtained by applying:

$$\frac{\text{Space width}}{\text{Line}} (\text{mm}) = \frac{1}{2 \times \text{LP}} = \frac{1}{10.08} = 0.099 \,\text{mm}$$

4 | RESULTS

The MA-XRF scanner has been tested for the non-destructive elemental imaging of the illumination of a $9 \times 11 \text{cm}^2$ juridical manuscript fragment from *liber xlvii* de publicis iudiciis. The small French oblong is dated ca. 1,300 and is now part of the special collection of the Northwestern Library. This object was chosen as a case study to test both the spatial resolution of the instrument in response to image small features and fine writing and comments as well as the instrument sensitivity to the subtle compositional changes associated with the different types of inks used to annotate this manuscript.

MA-XRF was performed with continuous scanning along the X direction. A fixed step-size of 300 μ m was selected along the Y direction. The X-ray source was operated at 30 kV and 0.4 mA. The total measurement time was 110 min. The open source PyMca software was used to batch fit the XRF results and to extract the elemental distribution maps presented in Figure 4. MA-XRF acquisition was complemented by RIS measurements to enhance pigment identification. The data have been recorded using a Resonon Pika II Pushbroom system in the 400–900 nm range with a spectral resolution of 2 nm and are presented in Figure 5.

Pb-based areas corresponding to lead white pigment are identified in the white outline of the illumination, lighter tones of the central character (e.g. in blue areas and in the small historiated initial), and flesh tones, as well as in very fine features such as small decorations within the frame of the illumination, and point-shaped contours around the circular motifs in the background. Using a visible microscope, the width of those features has been determined to be between 150 and 200 μm . These results confirm the appropriate resolution for allowing fast and relevant mapping of relatively fine features at the macroscale.

Pb-based painting material is also identified in the red garment of the left character and red part of the illuminated initial letter. With an inflection point around 565 nm, the reflectance spectrum collected in this area

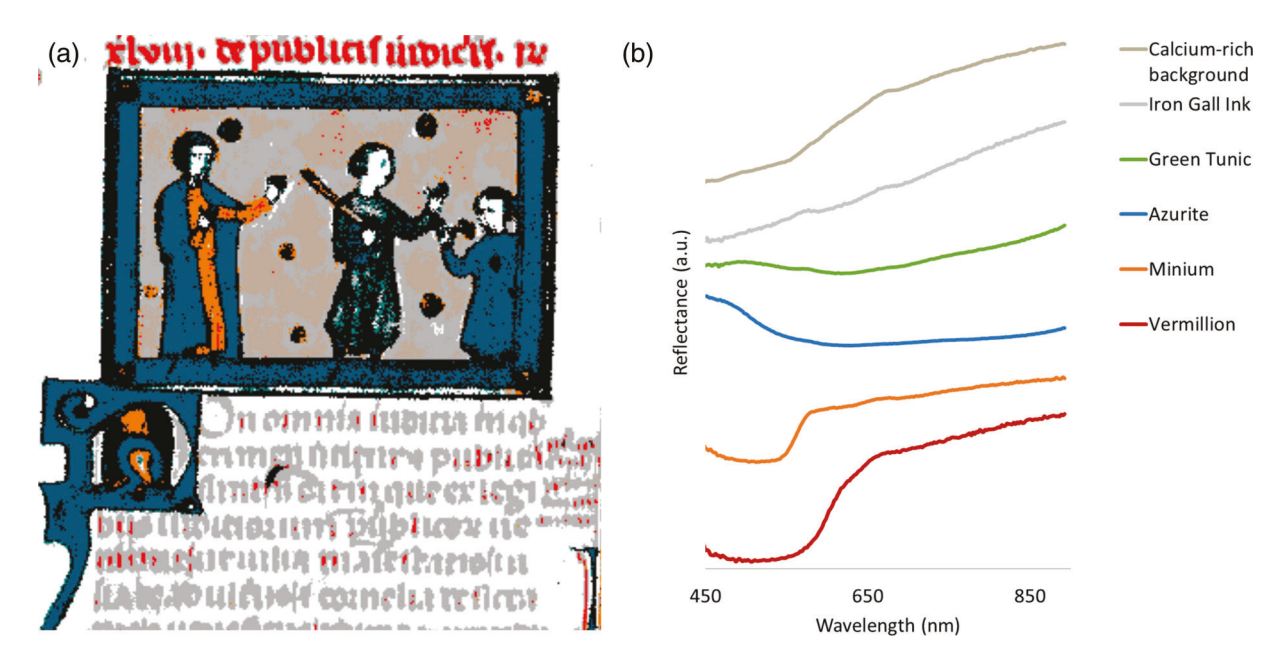


FIGURE 5 (a) RGB image obtained by Spectral Angle Mapper (from SpectrononPro) using the reference spectra presented in (b); (b) spectra of areas of reference determined using the approach detailed in Reference [18]; corresponding, respectively, to the use of vermillion, minium, azurite, and iron gall ink (the exact identification of the pigment used for the Cu-green tunic has not been determined by this study; however, a representative reflectance spectrum has been extracted from the dataset to identify its location). The same color code is used in both spatial and spectral representations (a) and (b)

confirms the presence of red lead (Pb_3O_4 , mineral form minium). MA-XRF confirmed the use of a Cu-based pigment in the blue tones of the illumination. With an absorption maximum around 640 nm and low reflectance in the red region, the presence of azurite ($2CuCO_3.Cu[OH]_2$) is revealed.

The presence of gold is confirmed in the gilded area of the illumination, with a strong correlation with the element calcium, pointing toward the use of a calcium-based preparation layer of the gilding area. Apart from the gilded area, calcium is identified in the background of the illumination; further work is, however, necessary

to provide an enhanced identification of the pigments used in this part of the manuscript.

Two types of ink are identified for the text and related annotations: one being rich in Fe (with traces of K), and another presenting a high ratio in Zn to Fe (together with Cu, Zn is a common component of iron-gall ink). The former ink has been used for the main text, while the annotations both in front and back of the miniature present the presence of Fe exclusively. For the red ink, Hg and S are correlated in MA-XRF maps. The reflectance spectra for the corresponding area reveal shapes similar to semiconductor pigments, that is, a sigmoid with a steeper rise

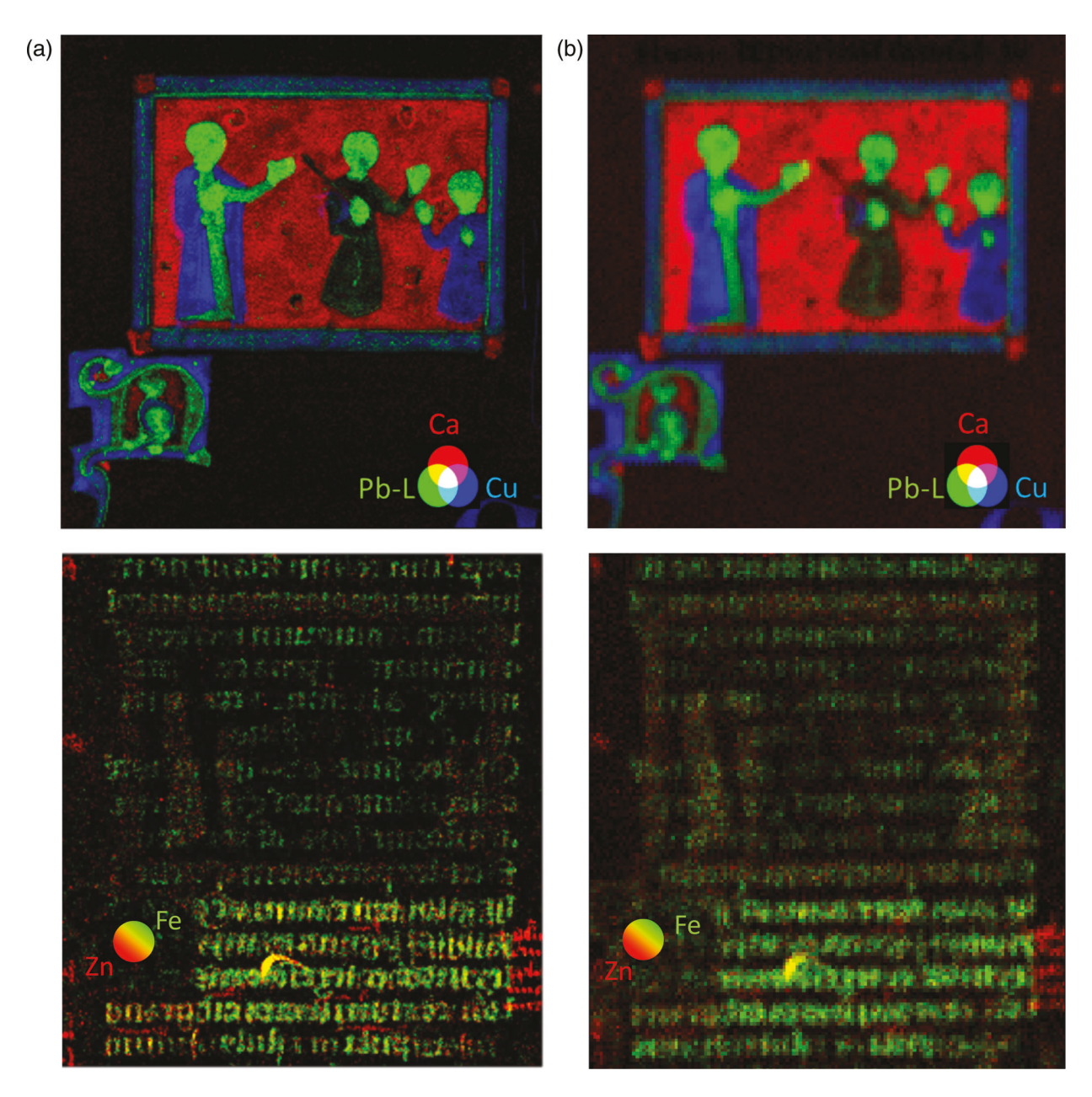


FIGURE 6 Comparison of the composite images of Ca K-, Cu K-, and Pb L-emission lines (top) and (bottom) Zn K- and Fe K-emission lines (right) of the illumination of the juridical manuscript fragment, acquired using (a) our in-house MA-XRF system and (b) the CRONO MA-XRF system

around the inflection point [33] at 590–605 nm that indicates the presence of vermillion (HgS). Here, again, the spatial resolution allows a distinct imaging and reading of the text.

The same manuscript was previously scanned using the CRONO system^[6] on loan to the Center for test purposes. The conditions used to scan the object were determined to provide the best information within the 2 hr time frame available with the object. Thus, the X-ray source was set to 50 kV, 0.2 mA and was equipped with a 0.5 mm collimator. These parameters allowed a sufficient signal-to-noise ratio (SNR) of the spectral information to run an acquisition with a 150 ms dwell time and a 500 µm pixel size (accounting for a 2 hr total acquisition time). The results obtained are presented in Figure 6 and are compared to the elemental maps obtained with our instrumentation. Whereas SNR between the two acquisitions were comparable for elements with Z < 40, elemental images obtained with similar acquisition times highlights the interest of using a focused beam to differentiate contour and fine features of the manuscript, thus providing additional information regarding pigment use.

5 | CONCLUSION

The first results obtained with our in-house macro-XRF scanner have been presented in this paper. The system is based on the experience gained with testing and using state-of-the-art MA-XRF equipment used in Cultural Heritage for the different projects undertaken at the Center.

The technical characteristics and spectrometric figures of merit of the scanner and elemental distribution images acquired on a historical illuminated manuscript have been presented. The resulting data confirm that the scanner satisfies the specifications required previously, as (a) it allows the detection of various elements within subsecond dwell times at sub-millimeter resolution; (b) it is transportable on site and for extensive travel, while presenting a straightforward and resilient mounting system; (c) it is versatile in terms of optic choices and acquisition modes, allowing multipurpose applications; and (d) it features a robust control software.

ACKNOWLEDGEMENTS

Victor Chou, Jean-Marie Rennetaud, and Erin Norwood from Hiwin are acknowledged for their support in developing an adapted scanning stage. Jared Sach from XOS is thanked for his design of the adaptive optical system. Scott Kraft, Curator of the Charles Deering McCormick Library of Special Collections, is thanked for providing access to the historical

manuscript. The Andrew W. Mellon Foundation is acknowledged for its support to the center for scientific studies in the arts. The center also received supplemental support from the Materials Research Center, the Office of the Vice President for Research, the McCormick School of Engineering and Applied Science, and the Department of Materials Science and Engineering at Northwestern University.

ORCID

Marc Walton https://orcid.org/0000-0002-4436-3546

REFERENCES

- [1] K. Janssens, G. Van der Snickt, F. Vanmeert, S. Legrand, G. Nuyts, M. Alfeld, L. Monico, W. Anaf, W. de Nolf, M. Vermeulen. Non-invasive and non-destructive examination of artistic pigments, paints, and paintings by means of X-ray methods, analytical chemistry for cultural heritage. Analytical Chemistry for Cultural Heritage. Topics in Current Chemistry Collections. Cham, Switzerland: Springer International, 2017, pp. 77–128. https://doi.org/10.1007/978-3-319-52804-5.
- [2] M. Alfeld, L. De Viguerie, Spectrochim. Acta B 2017, 136, 81–105.
- [3] M. Alfeld, J. V. Pedroso, M. van Eikema Hommes, G. van der Snickt, G. Tauber, J. Blaas, M. Haschke, K. Erler, J. Dik, K. Janssens. J. Anal. Atomic Spectrom. 2013, 28, 760–767.
- [4] E. Ravaud, L. Pichon, E. Laval, V. Gonzalez, M. Eveno, T. Calligaro, Appl. Phys. A 2016, 122, 17.
- [5] D. Strivay, M. Clar, S. Rakkaa, F.-P. Hocquet, C. Defeyt, *Appl. Phys. A* 2016, 122, 950.
- [6] R. Alberti, T. Frizzi, L. Bombelli, M. Gironda, N. Aresi, F. Rosi, C. Miliani, G. Tranquilli, F. Talarico, L. Cartechini, X-Ray Spectrom. 2017, 46, 297–302.
- [7] F. P. Romano, C. Caliri, P. Nicotra, S. di Martino, L. Pappalardo, F. Rizzo, H. C. Santos, J. Anal. Atomic Spectrom. 2017, 32, 773–781.
- [8] J. K. Delaney, D. M. Conover, K. A. Dooley, L. Glinsman, K. Janssens, M. Loew, Herit. Sci. 2018, 6, 31.
- [9] F. Vanmeert, W. De Nolf, S. De Meyer, J. Dik, K. Janssens, Anal. Chem. 2018, 90, 6436–6444.
- [10] P. Campos, C. Appoloni, M. Rizzutto, A. Leite, R. Assis, H. Santos, T. Silva, C. Rodrigues, M. Tabacniks, N. Added, Appl. Radiat. Isot. 2019, 152, 78.
- [11] M. Alfeld, K. Janssens, J. Dik, W. de Nolf, G. van der Snickt, J. Anal. Atomic Spectrom. 2011, 26, 899–909.
- [12] E. Pouyet, J. Delaney, K. Brummel, S. Webster-Cook, C. Dejoie, G. Pastorelli, M. Walton, SN Appl. Sci. 2020. (forthcoming).
- [13] E. Pouyet, S. Devine, T. Grafakos, R. Kieckhefer, J. Salvant, L. Smieska, A. Woll, A. Katsaggelos, O. Cossairt, M. Walton, Anal. Chim. Acta 2017, 982, 20–30.
- [14] G. Bertuccio, M. Ahangarianabhari, C. Graziani, D. Macera, Y. Shi, M. Gandola, A. Rachevski, I. Rashevskaya, A. Vacchi, G. Zampa, *IEEE Trans. Nuclear Sci.* 2016, 63, 400–406.
- [15] Retrieved from https://www.xglab.it/dpp-digital-pulseprocessor.shtml

- [16] V. Solé, E. Papillon, M. Cotte, P. Walter, J. Susini, *Spectrochim. Acta B* 2007, 62, 63–68.
- [17] J. K. Delaney, P. Ricciardi, L. D. Glinsman, M. Facini, M. Thoury, M. Palmer, E. R.d.l. Rie, Stud. Conserv. 2014, 59, 91–101.
- [18] E. Pouyet, N. Rohani, A. K. Katsaggelos, O. Cossairt, M. Walton, *Pure Appl. Chem.* 2018, 90, 493–506.
- [19] M. Alfeld, S. Pedetti, P. Martinez, P. Walter, CR Phys. 2018, 19, 625–635.
- [20] K. A. Dooley, E. M. Gifford, A. van Loon, P. Noble, J. G. Zeibel, D. M. Conover, M. Alfeld, G. Van der Snickt, S. Legrand, K. Janssens, *Herit. Sci.* 2018, 6, 1–15.

[21] A. Vandivere, A. van Loon, K. A. Dooley, R. Haswell, R. G. Erdmann, E. Leonhardt, J. K. Delaney, *Herit. Sci.* 2019, 7, 1–16.

How to cite this article: E Pouyet, N Barbi, H Chopp, et al. Development of a highly mobile and versatile large MA-XRF scanner for in situ analyses of painted work of arts. *X-Ray Spectrom*. 2021;50: 263–271. https://doi.org/10.1002/xrs.3173